ORIGINAL ARTICLE

Relationship between vessel diameter and depth measurements within the limbus using ultra-high resolution optical coherence tomography

Emmanuel Alabi [a], Natalie Hutchings [a], Kostadinka Bizheva [a,b,c], Trefford Simpson [a,*]

[a] University of Waterloo, School of Optometry and Vision Science, Waterloo, ON, Canada
[b] University of Waterloo, Department of Physics and Astronomy, Waterloo, ON, Canada
[c] University of Waterloo, Systems Design Engineering Department, Waterloo, ON, Canada

Abstract

Purpose: To establish a relationship between the diameter and depth position of vessels in the superior and inferior corneo-scleral limbus using ultra-high resolution optical coherence tomography (UHR-OCT).

Methods: Volumetric OCT images of the superior and inferior limbus were acquired from 14 healthy subjects with a research-grade UHR-OCT system. Differences in vessel diameter and depth between superior and inferior limbus were analyzed using repeated measured ANOVA in SPSS and R.

Results: The mean ($\pm$ SD) superior and inferior diameters were $29 \pm 18\,\mu$m and $24 \pm 18\,\mu$m respectively, and the mean ($\pm$ SD) superior and inferior depths were $177 \pm 109\,\mu$m and $207 \pm 132\,\mu$m respectively. The superior limbal vessels were larger than the inferior ones (RM-ANOVA, $p = 0.004$), and the inferior limbal vessels were deeper than the superior vessels (RM-ANOVA, $p = 0.041$). There was a positive linear association between limbal vessel depth and size within the superior and inferior limbus with Pearson correlation coefficients of 0.803 and 0.754, respectively.

Conclusion: This study demonstrated that the UHR-OCT was capable of imaging morphometric characteristics such as the size and depth of vessels in the limbus. The results of this study suggest a difference in the size and depth of vessels across different positions of the limbus, which may be indicative of adaptations to chronic hypoxia caused by the covering of the superior limbus by the upper eyelid. UHR-OCT may be a useful tool to evaluate the effect of contact lenses on the microvascular properties within the limbus.

© 2017 Spanish General Council of Optometry. Published by Elsevier España, S.L.U. This is an open access article under the CC BY-NC-ND license (http://creativecommons.org/licenses/by-nc-nd/4.0/).

* Corresponding author.
  E-mail addresses: ebalabi@uwaterloo.ca (E. Alabi), natalie.hutchings@uwaterloo.ca (N. Hutchings), kbizheva@uwaterloo.ca (K. Bizheva), trefford.simpson@uwaterloo.ca (T. Simpson).

Relación entre las mediciones del diámetro y la profundidad de vasos sanguíneos en el limbo obtenidas mediante tomografía de coherencia óptica de ultra-alta resolución

Resumen

Objetivo: Establecer la relación entre el diámetro y la profundidad de los vasos del limbo escle-rocorneal superior e inferior mediante tomografía de coherencia óptica de ultra-alta resolución (UHR-OCT).

Métodos: Se adquirieron 256 conjuntos de imágenes del limbo superior e inferior en 14 sujetos, mediante UHR-OCT. Se analizaron las diferencias en cuanto a diámetro y profundidad del vaso entre el limbo superior e inferior utilizando ANOVA de medidas repetidas en SPSS y R.

Resultados: Los diámetros medios ($\pm$ DE) superior e inferior fueron de 29 μm $\pm$ 18 μm y 24 μm $\pm$ 18 μm respectivamente, y las profundidades medias ($\pm$ DE) superior e inferior fueron de 177 μm $\pm$ 109 μm y 207 μm $\pm$ 132 μm respectivamente. Los vasos del limbo superior fueron de mayor tamaño que los del limbo inferior (RM-ANOVA, p = 0,004), y los vasos del limbo infe-rior fueron más profundos que los del limbo superior (RM-ANOVA, p = 0,041). Se produjo una asociación lineal positiva entre la profundidad y el tamaño del vaso dentro del limbo superior e inferior, con coeficientes de correlación de Pearson de 0,803 y 0,754, respectivamente.

Conclusión: Este estudio demuestra que UHR-OCT fue capaz de obtener imágenes de las carac-terísticas morfométricas tales como tamaño y profundidad de los vasos del limbo. Los resultados de este estudio sugieren una diferencia de tamaño y profundidad de los vasos en las diferentes posiciones del limbo, que puede ser indicativa de adaptaciones a la hipoxia crónica causada por el cubrimiento del limbo superior por parte del párpado superior. UHR-OCT puede ser una herramienta de utilidad para evaluar el efecto de las lentes de contacto sobre las propiedades microvasculares del limbo esclerocorneal.

Introduction

The limbus is the zone that separates the opaque sclera (overlaid by transparent conjunctiva) from the transparent cornea. It is a region of interest because it is a site of numerous biological activities ranging from supplying blood to the peripheral cornea, to housing the aqueous outflow apparatus.[1] The vascular properties of the limbus is impor-tant for many physiological responses such as nutrition, waste removal, and microvascular changes in response to corneal injury, inflammation or contact lens wear.[2] For most people, during both awake and asleep conditions, the superior limbus is covered by the upper eyelid; roughly two millimeters of the superior corneal region (the total area of the superior limbus) is obscured while the eye is in the open-eye primary-gaze position.[3] The lid is a barrier to atmospheric oxygen within the limbal zone and imme-diately after the retraction of the upper eyelid, superior corneal oxygen uptake is much higher than other parts of the cornea.[4–6] When equilibrated (after longer upper lid retraction) there is no difference in oxygen uptake of the various corneal regions.[7] When oxygen delivery to the limbus is reduced, limbal hyperemia occurs as blood flow is increased to the region.[8] Since limbal hyperemia is not the norm,[3] it can be deduced that anatomical and physiological alterations within the tissue might occur as a response to overcome the possible inadequate exposure to atmospheric oxygen that the superior limbus experiences as a result of it being constantly covered by the upper eyelid. Such adjustments in response to this chronic hypoxia might include but are not limited to, changes in vessel size, density and depth, as well as changes in epithelial thickness.

There are a number of other differences in the struc-tures of the upper limbus: The density of endothelial cells is greater in the superior limbus,[9] the diameters and spacing of collagen fibrils[10] and stem cell size[11] differ, and the superior cornea is thicker.[12,13] Because of these structural differ-ences and the coverage of the superior limbus by the upper eyelid, we examined some aspects of the vessel character-istics within the superior limbus and other limbal regions: Our working hypothesis was that there would be morpho-metric adaptations of the vessels that would provide some physiological accounting for the upper limbus not showing manifestations of chronic hypoxia.

Visualization of the limbus

Many methods exist for the visualization and morphometric analysis of structures within the limbus. Ex vivo tech-nology such as serial histologic sections[14,15] and ultrathin sections[16,17] have been used to visualize ocular vessels, trabecular meshwork and aqueous outflow in the limbus. Some shortcomings associated with this type of histological sectioning are that the curvature of the eye provides a barrier to the reconstruction of anatomical structures including vasculature, from sectioned materials, and the process cannot be carried out in vivo.[18]

In vivo methods of visualizing the limbus include but are not limited to slit lamp microscopy (SLB), gonioscopy, confocal microscopy, ultrasound biomicroscopy (UBM) and optical coherence tomography (OCT). In this study, OCT was utilized for visualization of the limbus particularly due to it being non-contact and non-invasive. It also provides high resolution cross-sectional images of optically scattering media and over the past 25 years has found numerous applications in ophthalmology for non-invasive imaging of different ocular tissues such as the retina, cornea, lens, etc. both in human subjects and animal models.[19] OCT has previously been used to image the human corneo-scleral limbus. Feng and Simpson,[20] utilized OCT to compare epithelial thickness within the central cornea and limbus. Kagemann et al.,[21] used OCT to assess the Schlemm's canal in the limbal region of 21 healthy and 3 glaucomatous subjects. Detailed three-dimensional mapping of limbal morphology has been carried out using ultra-high resolution OCT (UHR-OCT)[22] and further microstructural and microvascular limbal properties have been observed using a combination of anterior segment OCT and optical microangiography.[23] Imaging of both limbal and scleral vasculature has also been performed with swept source OCT.[24]

Due to the high level of biological activity within the ocular limbus, a repeatable in vivo, non-invasive and non-contact means of monitoring and measuring limbal structures at a high resolution might be beneficial as an aid to diagnosis and evaluation of anterior ocular conditions involving the various components of the limbus. The purpose of this study was to investigate morphometric characteristics of vasculature within the superior and inferior limbal regions using ultra-high resolution optical coherence tomography and compare the relationship between vessel diameter and depth within the human ocular limbus.

Methods

We used a research-grade high speed, spectral domain UHR-OCT operating at central wavelength of 1020 nm designed for in vivo imaging of the human anterior segment. The UHR-OCT system is based on a fiber-optic Michelson interferometer powered with a broadband superluminescent diode (SLD – Superlum Inc.). The SLD generates a spectrum centered at 1020 nm with spectral bandwidth of 110 nm. The optic and fiber-optic components of the UHR-OCT system were selected to propagate the SLD spectrum through the entire UHR-OCT system with no significant spectral losses. The detection end of the UHR-OCT system consists of a high resolution custom spectrometer (P&P Optica, Waterloo, Canada) interfaced with a 1024 pixel, line IR camera (LDH, UTC Aerospace Systems, Westford, MA, USA) operating at 47 kHz. The UHR-OCT system provided 4.2 μm axial resolution in free space, corresponding to ∼3 μm in biological tissue assuming an average refractive index of 1.38. The corneal imaging probe used for this study generated lateral resolution of ∼18 μm in biological tissue. The UHR-OCT system provided ∼92 dB SNR for 1.4 mW power of the imaging beam incident on the cornea and conjunctiva, which is in compliance with the safety limits established by the ANSI standard for safe exposure of ocular tissue to laser light. More details about the design of the UHR-OCT system are provided in previous publications from our research group.[22,25,26] For imaging the anterior structures of the human eye, an UHR-OCT system operating in the 1060 nm spectral range has a major advantage over similar systems operating at 800 nm or 1300 nm; the dispersion of water has a null at ∼1060 nm and provided that the optical dispersion within the UHR-OCT imaging system is balanced, the images acquired do not require post-processing for water dispersion compensation.[22] Also, devices operating at the 1060 nm range are more suited for the imaging anterior segment structures as they provide greater depth penetration in more scattering biological tissue such as the limbus, sclera, eyelid, etc., as compared to devices operating in the 800 nm range.[22,27]

Participants

14 healthy non-contact lens wearers between the ages of 16–60 years were used in the study. Imaging was done after midday to reduce the influence of diurnal variation.[28] There was no dietary exclusion criteria since we were interested in examining the vessels in as unselected a way as possible. Prior to imaging, participants' ocular health was assessed and informed consent was obtained. This study adhered to the Declaration of Helsinki for research involving human subjects and received ethics approval from the University of Waterloo Office of Research Ethics. Imaging with the UHR-OCT device was carried out on the participants while their upper or lower eyelids were manually retracted and while they fixated on a target inferiorly and superiorly, for upper and lower limbus imaging respectively. Head position remained relatively stable as the subject was comfortably positioned in a chin and forehead rest. Based on a specular reflection, the UHR-OCT imaging probe was approximately orthogonally aligned to the subject's eye to allow for the acquisition of 256 cross-sectional images (1000 × 1024) of the corneo-scleral limbus.

Data processing and analysis

All UHR-OCT tomograms were processed with Matlab (Math-works), Amira (Visage Imaging) and Image J.[29] 8 bit image stacks (1000 × 1024 × 256) were acquired of the transition from clear cornea to bulbar conjunctiva at the superior and inferior limbal region. To facilitate definitions of vessels (particularly those with low contrast), sets of images were registered into a stack using a standard translation transformation[30] and 3D construction of the aligned stack was done using Amira and ImageJ. Then to define the limbal region, an orthogonal line was drawn on the image, from the termination of the Bowman's-epithelium complex through the termination of the endothelium-Decemet's complex. This denoted the corneo-limbal junction, while a line orthogonal to the ocular surface though the furthermost insertion of the sclera to the anterior chamber denoted the sclera-limbal junction. The area that fell within these two borders was presumed to be the limbal zone (Fig. 1).

A single 2D image/section of the limbal region was selected as the candidate image for blood vessel evaluation. This was located near the position of orthogonal illumination and was selected on the basis that all layers from 'front to back' were in focus. On this 2D section, the diameters of
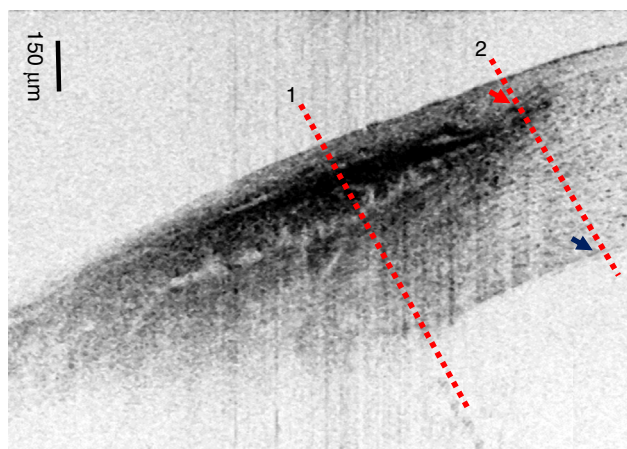
150 μm

Figure 1 OCT image showing the corneo-scleral limbus. The red arrow shows the termination of the epithelium-Bowman's complex. The blue arrow shows the termination of the Descemet's-endothelial complex. The red dashed line 1 shows the sclero-limbal junction and red dash line 2 shows the corneo-limbal junction. The area between the two lines is the limbal region.

all visible vessels within the limbal region were measured using a circle or ellipse tool, the shorter diameter in the case of an ellipse tool. The vessel depth was quantified as the orthogonal/shortest distance from the ocular surface to the outer vessel boundary.

Pearson correlation coefficients were calculated to investigate the anatomical relationship between vessel diameter and depth. Quantitative differences in vessel size and depth in the limbal region were analyzed using repeated measured ANOVA. R[31] and SPSS for Windows[32] were used for data analysis procedures. A probability value of 0.05 or less was assumed to be significant.

Results

Morphometry and quantitative differences

The morphometric characteristics of vessels with the superior and inferior limbus can be found in Tables 1 and 2 respectively. The average vessel size (in microns) for superior and inferior limbus were 29 ± 18 (SD) and 24 ± 18 (SD) respectively. The average vessel depths for superior and inferior limbus were 177 ± 109 (SD) and 206 ± 132 (SD) respectively. Fig. 2 contains information about the vessel diameter and depth found at both the superior and inferior limbus. The vessels within the superior limbus were larger than the vessels found in the inferior limbus (RM-ANOVA, $p = 0.004$) and those within the inferior limbus were on average deeper than the vessels found within the superior limbus (RM-ANOVA, $p = 0.041$).

Associations

There were positive linear relationships between limbal vessel depth and size within the superior and inferior limbus (Fig. 4). The Pearson correlation coefficients for the superior and inferior limbus were 0.803 and 0.754 respectively. The within subject Pearson correlation coefficients are displayed in Fig. 3 for the superior and inferior limbus.

Discussion

In this study, we were able to reliably image, obtain and quantify vascular morphometric characteristics in the human corneo-scleral limbus. Our research supports the utility of the UHR-OCT in anterior segment imaging to be beneficial for evaluation of various components of the vascularity of the limbus. Since there is little published work on the test and retest reliability of OCT measurements

Table 1 Morphometric characteristics for the superior limbal region.

Subject	Age (years)/sex (male-M)/(female-F)	Ethnicity	Vessel diameter (μm)		Vessel depth (μm)		# of vessels
			Mean value ± SD	Min–Max values	Mean value ± SD	Min–Max values	
1	28/M	White	25 ± 17	8–52	230 ± 145	75–519	8
2	30/M	Asian	16 ± 10	6–38	167 ± 105	47–417	10
3	42/M	White	25 ± 19	7–70	189 ± 156	57–550	10
4	24/M	White	19 ± 14	5–55	200 ± 111	92–464	13
5	29/F	Black	22 ± 17	5–55	199 ± 108	117–483	13
6	34/M	Black	35 ± 27	9–116	269 ± 136	50–531	15
7	34/M	Asian	19 ± 15	6–63	205 ± 166	56–527	18
8	32/F	White	20 ± 13	7–64	215 ± 123	57–568	17
9	29/F	White	28 ± 17	10–63	219 ± 187	57–591	12
10	28/F	Black	29 ± 22	7–77	194 ± 89	82–440	15
11	35/F	White	23 ± 21	6–73	204 ± 126	64–505	13
12	55/M	Asian	19 ± 13	6–38	173 ± 91	66–374	9
13	42/M	White	27 ± 17	6–55	182 ± 129	53–400	12
14	26/F	White	25 ± 21	9–64	211 ± 182	49–642	8

Table 2 Morphometric characteristics for the inferior limbal region.

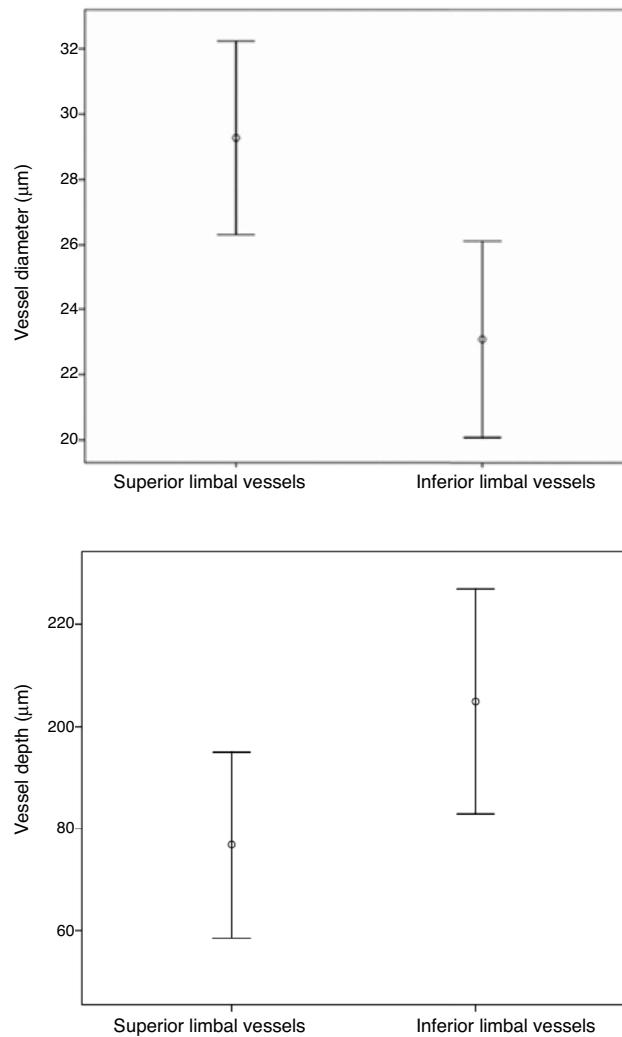| Subject	Age (years)/sex (male-M)/(female-F)	Ethnicity	Subject	Vessel diameter (μm)		Vessel depth (μm)		# of vessels
				Mean value ± SD	Min–Max values	Mean value ± SD	Min–Max values	
1	28/M	White	1	25 ± 17	8–52	230 ± 145	75–519	8
2	30/M	Asian	2	16 ± 10	6–38	167 ± 105	47–417	9
3	42/M	White	3	25 ± 19	7–70	189 ± 156	57–550	10
4	24/M	White	4	19 ± 14	5–55	200 ± 111	92–464	12
5	29/F	Black	5	22 ± 17	5–55	199 ± 108	117–483	13
6	34/M	Black	6	35 ± 27	9–116	269 ± 136	50–531	15
7	34/M	Asian	7	19 ± 15	6–63	205 ± 166	56–527	18
8	32/F	White	8	20 ± 13	7–64	215 ± 123	57–568	17
9	29/F	White	9	28 ± 17	10–63	219 ± 187	57–591	12
10	28/F	Black	10	29 ± 22	7–77	194 ± 89	82–440	15
11	35/F	White	11	23 ± 21	6–73	204 ± 126	64–505	13
12	55/M	Asian	12	19 ± 13	6–38	173 ± 91	66–374	9
13	42/M	White	13	27 ± 17	6–55	182 ± 129	53–400	12
14	26/F	White	14	25 ± 21	9–64	211 ± 182	49–642	8

Figure 2 (Above) Superior and inferior limbal mean vessel diameters. (Below) Superior and inferior limbal mean vessel depths. The error bars show the 95% confidence interval of the mean.
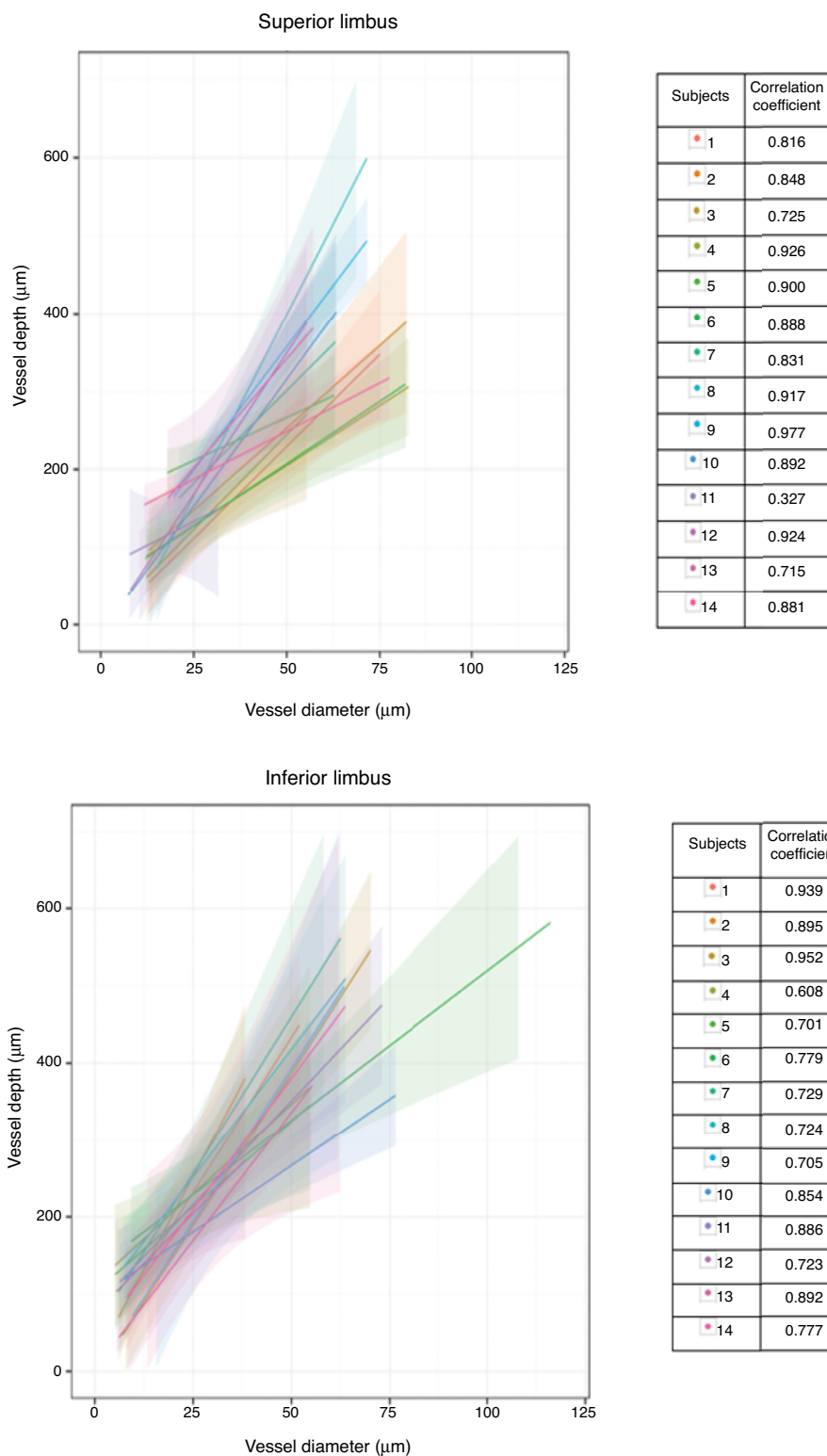
Superior limbus

Subjects	Correlation coefficient
1	0.816
2	0.848
3	0.725
4	0.926
5	0.900
6	0.888
7	0.831
8	0.917
9	0.977
10	0.892
11	0.327
12	0.924
13	0.715
14	0.881

Inferior limbus

Subjects	Correlation coefficient
1	0.939
2	0.895
3	0.952
4	0.608
5	0.701
6	0.779
7	0.729
8	0.724
9	0.705
10	0.854
11	0.886
12	0.723
13	0.892
14	0.777

Figure 3   Subject-wise regressions illustrating the relationships between vessel depth and diameter in the superior limbus (above) and in the inferior limbus (below).

on vessel characteristics within the limbus, we incorporated a component of repeatability. Initial vessel depth and size measurements were recorded within a 24-h period. The vessel depth and size were re-measured and recorded after a 60-day interval. The UHR-OCT was capable of imaging

limbal morphometric characteristics in a repeatable manner (Table 3).

Morphometric characteristics of limbal vessel diameter and depth are important. First, they provide information about the function of the vessels[34] and give further
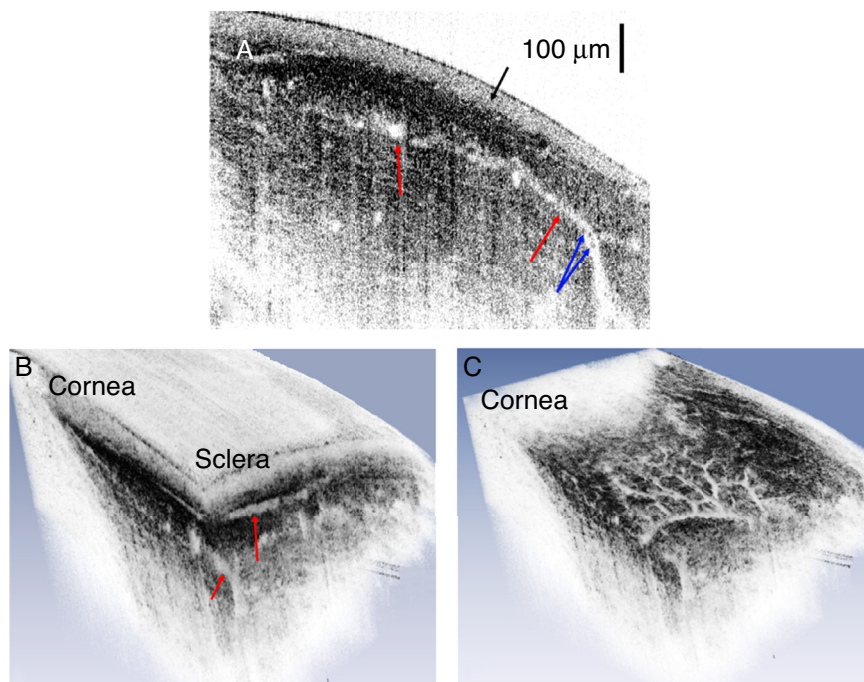
Figure 4 (A) Representative OCT B-scan of a healthy human corneo-scleral limbus. Black arrow marks the conjunctiva. Red arrows mark limbal blood vessels. Blue arrows mark individual red blood cells in the major scleral blood vessel. (B) Three dimensional reconstruction of a set of UHR-OCT tomograms. This reconstruction can be sliced at different angles and the vessels assessed and measured with the requisite ellipse or circle tool. Red arrows mark cross-sections of scleral blood vessels. (C) Three dimensional reconstruction of the limbus with the epithelium stripped through an oblique slice to reveal the vessel structure within the limbus. In (B) and (C) the images were black/white inverted so that the limbal voids being mapped appear as white against a dark background to allow enhanced viewing for readers.

Table 3 Relationship between replicate measures of vessel diameter and vessel depth of vessels in the image. The table describes the mean difference in repeated measurement, the 95% confidence interval for the mean difference (95% CI Mean), the upper limit of agreement (upper LOA), the lower limit of agreement (lower LOA), and the coefficient of repeatability (CR). Confidence intervals on the LOAs are determined using the method described by Carkeet.[33]

Measure	Mean diff.	95% CI mean diff.	Upper LOA	95% CI upper LOA	Lower LOA	95% CI lower LOA	CR
Inferior diameter	+0.17	−1.81 to +2.1	+4.22	+3.85 to +4.72	−3.89	−3.51 to −4.38	2.07
Superior diameter	+0.05	−1.92 to +2.03	+11.10	+9.97 to +12.63	−11.00	−9.87 to −12.53	5.62
Inferior depth	−1.28	−3.25 to +0.70	+16.50	+14.85 to +18.66	−19.05	−17.39 to −21.21	9.13
Superior depth	+0.26	−1.72 to +2.24	+13.08	+11.77 to +14.85	−12.57	−11.25 to −14.34	6.53

insight into the anatomical/physiological properties within the limbus.[1] An understanding of the morphometry in the limbal region is of further importance in ocular pathophysiology, for example, the microvascular changes that occur during and after contact lens wear.[35,36] While the changes that occur in the cornea after contact lens wear have been very well documented, there is little knowledge about the effect of contact lens wear on morphometric microvascular properties within the limbus. Studies have shown increase in limbal redness[35] and significant neovascularization within the limbus after extended contact lens wear,[36] our imaging technique would thus provide a quantitative means of assessing these limbal morphometric changes. Other applications where quantitative characterization of the vessels in the limbus would be beneficial include vessel changes (size,

tortuosity, neovascularization, etc.) in response to ocular surface injury, infection and inflammation.

The morphometric findings of this study suggest that the vessels found in the superior limbus are on average larger (have greater diameter) and are closer to the ocular surface than the vessels located within the inferior limbus. In support of this finding, there appears to be greater demand for oxygen in the region around the superior limbus,[4,5,7] and this could be a reason for the difference in vessel sizes within the two limbal regions. The difference in vessel size between the superior and inferior limbus may very well be an adaptation to the chronic hypoxia caused by the upper eyelid's constant coverage of the superior limbus.[37]

It is important to mention that though we have focused on hypoxia as being a primary difference between the upper

limbus and other corneal areas not covered by the lid, there are other putative differences that alone or in combination with any of the others might contribute to structural and/or physiological differences that might impact vascularity under the lid. These would include mechanical effects of the lid on the tissue, the effect of the lid in occluding illumination (in particular, perhaps, UV), differences in the chemistry of the tear film, and thermal effects. Since, unfortunately, we are not able to systematically assess the contributions of these variables, at least for the time being, we can only speculate that they might play a role in regional corneal, conjunctival and scleral tissue differences: This is not any different than our speculation about the effect of the lid inducing relative hypoxia.

There were some limitations to our study. For our experiment, a refractive index of 1.376 was assumed for the entire corneo-limbal region. It is important to note that a variation in refractive index both axially and across the cornea has previously been reported.[38] Since we did not adopt these variations to adjust the images from which measurements were made there might be minor variations of our measurements compared to, say, histological measurements. In addition to this challenge, vessel contents do not have the same refractive index; this might also contribute minor errors in the transitioning from optical thickness measures to physical thickness. Since we were relatively unselective in our sampling as far as controlling potential covariates that might have influenced vessel diameter is concerned (e.g. stimulants in the diet), it is possible that vessel diameter (but presumably not vessel depth) might have been influenced by these sorts of factors. Nevertheless, within participants and on average, the relationship between diameter and depth was similarly linear, and although the slopes of the functions illustrated in Fig. 3 might have been different because of, say, a dietary vaso-constrictor or vaso-dilator, the *linearity* of the relationships would not have been expected to be altered (although the regression intercept but not the regression slopes might have been expected to be different).

The sample size was not large and one might argue that the differences between participants was large (or one might also argue that the difference between participants was small). Unfortunately, with a new metric, there is little to go on in making judgements about variability. What we were able to determine, however, was that despite the between subject variability, the difference in mean vessel size and depth statistically differed with location (a calculation based both on the mean difference as well as the variability between participants). A larger sample size or less variability between participants would not theoretically alter this, other than making it less likely that we would be rejecting the null hypothesis in error (i.e., making a type I error).

Finally, the vasculature of the corneo-scleral limbus consists of both blood and lymph vessels. Because the ranges of blood and lymph vessels diameters overlap and the fact that our study employed only morphological OCT imaging, it was not possible to distinguish between blood and lymph vasculature in from the OCT data. Because blood and lymph flow have different velocities, it may be possible to identify blood and lymph vessels in OCT images by employing a Doppler OCT protocol. The OCT instrument used in our study is capable of executing a Doppler OCT imaging protocol. However, there are several potential challenges: first, lymph is far less scattering than red blood cells in the 1060 nm spectral range (the operation wavelength of OCT instrument used in our study), which means that the Doppler signal from lymph vessels will be close to the noise level. Second, lymph and blood flow velocities in vessels are dependent on the vessel size and viscosity of the flowing fluid. Blood flow in capillaries has rates similar to that of large lymph vessels, therefore identifying blood and lymph vessels based purely on frequency Doppler shift would generate unreliable data and can lead to incorrect conclusions.

For these reasons, we chose to adopt the term ''vasculature'' throughout our manuscript without specifying blood or lymph vessels. It is evident that this limits the findings of this study to its utility in aqueous related applications such as glaucoma pathophysiology. However, in relation to the earlier mentioned applications (tracking limbal vessel changes in response to contact lens wear corneal injury or infection, and identifying and quantifying neovascularization in limbus) our technique is a valid and useful tool.

Conclusion

The results from this study primarily indicate that vessel depth and diameter within the human limbus can effectively be imaged and measured in vivo using UHR-OCT, even under the lid where details might be obscured with conventional methods (e.g., a slit lamp biomicroscope). In addition, with protocols controlling imaging procedures (e.g., optical and structural alignment) and automated measurement tools, these measurements are repeatable. There are linear associations between vessel diameter and depth in both the upper and lower limbus and together with their quantitative differences it can be suggested that the relatively hypoxic environment under the upper lid contributes to vessels in the superior limbus being relatively larger and closer to the ocular surface than those within the inferior limbus. UHR-OCT can be a useful tool in evaluating changes to the microvascular properties that may occur within the limbus after contact lens wear.

Conflicts of interest

The authors have no conflicts of interest to declare.

Acknowledgements

References

1. van der Merwe EL, Kidson SH. Advances in imaging the blood and aqueous vessels of the ocular limbus. *Exp Eye Res*. 2010;91:118–126.
2. Efron N, Jones L, Bron AJ, et al. The TFOS International Workshop on Contact Lens Discomfort: report of the contact lens interactions with the ocular surface and adnexa subcommittee. *Investig Ophthalmol Vis Sci*. 2013;54:TFOS98-122.

3. Oyster CW. *The Human Eye: Structure and Function*. Sunderland, Mass: Sinauer Associates; 1999.

4. Benjamin WJ, Hill RM. Human cornea: superior and central oxygen demands. *Graefe's Arch Clin Exp Ophthalmol*. 1988;226:41–44.

5. Benjamin WJ, Rasmussen MA. Oxygen consumption of the superior cornea following eyelid closure. *Acta Ophthalmol*. 1988;66:309–312.

6. Fitzgerald J, Efron N. Oxygen uptake profile of the human cornea. *Clin Exp Optom*. 1986;69:149–152.

7. Benjamin WJ, Ruben CM. Human corneal oxygen demands at superior, central, and inferior sites. *J Am Optom Assoc*. 1995;66:423–428.

8. Papas E. The role of hypoxia in the limbal vascular response to soft contact lens wear. *Eye Contact Lens: Sci Clin Pract*. 2003;29. S72-4; discussion S83-4, S192-4.

9. Amann J, Holley G, Lee S, Edelhauser H. Increased endothelial cell density in the paracentral and peripheral regions of the human cornea. *Am J Ophthalmol*. 2003;135:584–590.

10. Boote C, Dennis S, Newton R, Puri H, Meek K. Collagen fibrils appear more closely packed in the prepupillary cornea: optical and biomechanical implications. *Investig Ophthalmol Vis Sci*. 2003;44:2941–2948.

11. Romano AC, Espana EM, Yoo SH, Budak MT, Wolosin JM, Tseng SC. Different cell sizes in human limbal and central corneal basal epithelia measured by confocal microscopy and flow cytometry. *Investig Ophthalmol Vis Sci*. 2003;44: 5125–5129.

12. Liu Z, Huang A, Pflugfelder S. Evaluation of corneal thickness and topography in normal eyes using the Orbscan corneal topography system. *Br J Ophthalmol*. 1999;83:774–778.

13. Liu Z, Xie Y, Zhang M. Corneal topography and pachymetry in normal eyes. *Zhonghua Yan Ke Za Zhi*. 2001;37: 125–128.

14. Hamanaka T, Bill A, Ichinohasama R, Ishida T. Aspects of the development of Schlemm's canal. *Exp Eye Res*. 1992;55:479–488.

15. Krohn J, Bertelsen T. Light microscopy of uveoscleral drainage routes after gelatine injections into the suprachoroidal space. *Acta Ophthalmol Scand*. 1998;76:521–527.

16. Bron A, Tripathi R, Tripathi B, Wolff E. *Wolff's Anatomy of the Eye and Orbit*. London: Chapman & Hall Medical; 1997.

17. Smith R. Haploinsufficiency of the transcription factors FOXC1 and FOXC2 results in aberrant ocular development. *Hum Mol Genet*. 2000;9:1021–1032.

18. Burger PC, Chandler DB, Fryczkowski AW, Klintworth GK. Scanning electron microscopy of microcorrosion casts: applications in ophthalmologic research. *Scan Microsc*. 1987;1:223–231.

19. Drexler W, Fujimoto J. *Optical Coherence Tomography*. Berlin: Springer; 2008.

20. Feng Y, Simpson T. Comparison of human central cornea and limbus in vivo using optical coherence tomography. *Optom Vis Sci*. 2005;82:416–419.

21. Kagemann L, Wollstein G, Ishikawa H, et al. Identification and assessment of Schlemm's canal by spectral-domain optical coherence tomography. *Investig Ophthalmol Vis Sci*. 2010;51:4054–4059.

22. Bizheva K, Hutchings N, Sorbara L, Moayed A, Simpson T. In vivo volumetric imaging of the human corneo-scleral limbus with spectral domain OCT. *Biomed Opt Exp*. 2011;2:1702–1794.

23. Li P, An L, Reif R, Shen T, Johnstone M, Wang R. In vivo microstructural and microvascular imaging of the human corneo-scleral limbus using optical coherence tomography. *Biomed Opt Express*. 2011;2:3109–3118.

24. Grulkowski I, Liu JJ, Baumann B, Potsaid B, Lu C, Fujimoto JG. Imaging limbal and scleral vasculature using swept source optical coherence tomography. *Photonics Lett Pol*. 2011;3:132–134.

25. Sorbara L, Simpson T, Maram J, Song E, Bizheva K, Hutchings N. Optical edge effects create conjunctival indentation thickness artefacts. *Ophthalmic Physiol Opt*. 2015;35:283–292.

26. Bizheva K, Lee P, Sorbara L, Hutchings N, Simpson T. In vivo volumetric imaging of the human upper eyelid with ultrahigh-resolution optical coherence tomography. *J Biomed Opt*. 2010;15:0405–408.

27. Steinert R, Huang D. *Anterior Segment Optical Coherence Tomography*. Thorofare, NJ: SLACK; 2008.

28. Thompson B, Read SA, Dumoulin SO, et al. Imaging the visual system: from the eye to the brain. *Ophthalmic Physiol Opt*. 2016;36:213–217.

29. Rasband W, Image JU. *National Institutes of Health*. Maryland, USA: Bethesda; 2014.

30. Thevenaz P, Ruttimann U, Unser M. A pyramid approach to sub-pixel registration based on intensity. *IEEE Trans Image Process*. 1998;7:27–41.

31. R Core Team. *R: A Language and Environment for Statistical Computing*. Vienna, Austria: R Foundation for Statistical Computing; 2012. ISBN:3-900051-07-0 http://www.R-project.org/.

32. SPSS Inc. Released 2007. SPSS for Windows, Version 16.0. Chicago, SPSS Inc.

33. Carkeet A. Exact parametric confidence intervals for Bland–Altman limits of agreement. *Optom Vis Sci*. 2015; 92:71–80.

34. Papas EB. The limbal vasculature. *Contact Lens Anterior Eye*. 2003;26:71–76.

35. McMonnies CW, Chapman-Davies A, Holden BA. The vascular response to contact lens wear. *Optom Vis Sci*. 1982;59:795–799.

36. Dumbleton KA, Chalmers RL, Richter DB, Fonn D. Vascular response to extended wear of hydrogel lenses with high and low oxygen permeability. *Optom Vis Sci*. 2001;78:147–151.

37. Baum JL. Prolonged eyelid closure is a risk to the cornea. *Cornea*. 1997;16:602–611.

38. Vasudevan B, Simpson TL, Sivak JG. Regional variation in the refractive-index of the bovine and human cornea. *Optom Vis Sci*. 2008;85:977–981.